Chimica Techno Acta
published by Ural Federal University
eISSN 2411-1414
chimicatechnoacta.ru

ARTICLE
2023, vol. 10(1), No. 202310105
DOI: 10.15826/chimtech.2023.10.1.05

Synthesis and characterization of ZnBTC-based MOFs: effect of solvents and salts

Maria V. Timofeeva *, Andrey N. Yankin

School of Physics and Engineering, ITMO University, St. Petersburg 197101, Russia
* Corresponding author: maria.timofeeva@metalab.ifmo.ru

This paper belongs to the MOSM2022 Special Issue.

Abstract

In this work, we studied the optimization of synthetic approaches to creating structurally modified metal-organic frameworks under various synthesis conditions. We investigated the influence of the various solvents and zinc salts on the structural characteristics of the metal-organic framework based on benzene-1,3,5-tricarboxylic acid (H_3BTC). The results indicate that the variation of the types of both solvent and salt is a parameter affecting the crystallinity, phase purity, and morphology of the metal-organic framework. This was confirmed by comprehensive structural characterization (SEM, EDX, PXRD).

Keywords

metal-organic frameworks
solvothermal synthesis
trimesic acid
MOF synthesis

Received: 11.11.22
Revised: 13.12.22
Accepted: 13.12.22
Available online: 22.12.22

Key findings

- The synthesis method for obtaining ZnBTC.
- New morphology of ZnBTC not previously described in the literature was obtained.
- It was found that the type of solvents and the type of salts used in the synthesis of the ZnBTC affect the morphology of the compounds.

1. Introduction

Materials have always played an important role in the development of humanity. The past 20 years have been marked by major achievements in the theoretical and applied materials science, which continues to develop rapidly. The main directions of modern materials science are as follows: a) polyfunctionality – giving the material the maximum number of different useful properties; b) the use of nano-sized materials; c) creation of smart materials capable of changing their characteristics under the effect of various external factors (light, temperature, electromagnetic field, etc.).

Currently, various materials have been intensively studied in materials science, such as inorganic nanoparticles [1–3], molecular crystals [4–6], COF (covalent organic framework) [7, 8]. Applications for these materials include electronics [9], cancer treatment [10], catalysis [11], etc.

Porous materials attract special attention in materials science. Porous materials are solids with voids filled with air or other gases. Porous materials can be ordered (crystalline, with a regular pore system) and disordered (irregular pores system). Inorganic materials often have a highly ordered structure, whilst plastics, for example, are amorphous or partially ordered.

Amorphous materials have certain advantages: they are inexpensive and easy to process. Their disadvantage is the uncertainty of the structure (due to the difficulties in X-ray diffraction analysis). Their synthesis is most often unpredictable; they exist in the form of several modifications and have low mechanical strength.

More interesting are the highly ordered materials, the structure of which can be studied by X-ray diffraction methods. These are, for example, crystalline zeolites [12, 13]. They have a regular structure, are strong, and possess the ion exchange capability. Their main applications are is molecular sieves and catalysts [14–16]. The development of a new class of highly ordered hybrid structures – metal-organic frameworks – is the next stage in the development of zeolite-like materials.

Metal-organic framework (MOF) are a class of crystalline porous coordination compounds with a 1-, 2-, 3-dimensional structure consisting of metal ions or clusters linked by organic linkers [17–21]. Different functionality, adjustable porosity, mechanical strength and thermal stability can be

imparted to the framework by changing its constituent parts [22]. Due to these properties MOF appear as promising materials that can be used for the adsorption/storage and separation of gases, in catalysis, biomedicine, and also for the creation of sensor devices [23–26]. Of particular interest is the further modification of the structure of MOFs, including their intracrystalline space, to create new properties or optimize existing structural/chemical characteristics [27,28].

However, there are just a few studies that demonstrate the conditions for the MOFs synthesis effect on the structure and properties of the framework. The comprehensive understanding of the framework's synthesis and formation and its effect on the final structure are still missing [29–31].

Among the ligands for the synthesis of MOFs, trimesic acid has a leading position. Thus, the most famous and one of the first MOFs, HKUST-1, is based on trimesic acid and copper salt [32, 33]. Trimesic acid and its derivatives are available and ecofriendly substances that can be used as intermediate pharmaceutical products and as drug delivery agents as parts of MOF [34, 35]. There are many publications on MOFs based on Ni [36], Fe [37], Co [38, 39] and other metals [40], where trimesic acid played the role of a ligand [41–43]. Basically, these publications investigated the possible applications MOF: catalysis [44–46], medicine [47, 48], adsorption [49–51], sensors [52–53]. However, to the best of our knowledge, there is no research on the development of a synthesis strategy and design of BTC-based MOFs.

Nowadays, there are different methods for MOFs production: solvothermal (synthesis under high pressure, in a boiling solvent), microwave (synthesis by radiation of a microwave explosion), sonochemical (synthesis under the action of ultrasound), microfluidic (control of liquid flows at micro- and nanoscales), mechanochemical, electrochemical and slow evaporation method (does not require any traces, electricity or mechanical action). Consequently, there is often a discrepancy in the structural data between different reports on the same MOF, which usually arises from using different methods and parameters of synthesis.

ZnBTC is a well-known MOF in which infinite zinc chains are connected by organic ligand into a three-dimensional microporous framework [54]. Despite only one synthesis method, there are various ZnBTC morphologies known, which can be explained by different conditions of the solvothermal reaction. Among existing morphologies, nonuniform rod-like [55], large crumps with irregular shapes [56], and spherical nanoparticle [57, 58] structures of ZnBTC can be distinguished. It is important to mention that all known methods for the synthesis of ZnBTC take place at high temperatures (>120 °C).

Here we report the optimization of the MOFs synthesis based on zinc salt and trimesic acid. We studied the critical role of the solvent type variation on the morphology and crystallinity of the synthesized MOF based on zinc salt. We report the soft synthesis conditions (80 °C temperature). In this regard, the following adjustments to the synthesis technique were attempted: a) variation of the solvent mixture; b) precursor (zinc salt type) variation.

2. Experimental

All the chemical reagents were obtained from commercial sources and used without further purification unless otherwise specified: $Zn(NO_3)_2 \cdot 6H_2O$ (Sigma-Aldrich, ≥98.0%), $ZnSO_4 \cdot 7H_2O$ (Sigma-Aldrich, ≥98.0%), $Zn(CH_3CO_2)_2 \cdot 2H_2O$ (Sigma-Aldrich, ≥98.0%), 1,3,5-benzenetricarboxylic acid (Sigma-Aldrich, Trimesic acid (H3BTC), 95%), dimethylformamide (ACS reagent, ≥99.8%), ethanol (ACS reagent, ≥99,5%), 1,4-dioxane (Dioxane, ACS reagent, ≥99,5%), ethanol (EtOH, ACS reagent, ≥ 99,5%), toluene (Tol, ACS reagent, ≥99,5%), chlorobenzene (PhCl, ACS reagent, ≥99,5%), and dimethyl sulfoxide (DMSO, ACS reagent, ≥99,5%) were used in all syntheses.

The chemical composition and homogeneity of obtained compounds were controlled with a scanning electron microscope (SEM, Quanta 200, FEI, Netherlands) with an accelerating voltage of 10 kV. Dry samples were coated with a gold thin film and imaged with SEM.

Diffraction patterns of the samples were recorded on a Shimadzu 7000-maxima X-ray diffractometer with a 2 kW characteristic Cu Kα (Kα1 λ = 1.54059 Å, angular range 2θ = 5° – 80°) X-ray radiation source and a Bragg-Brentano goniometer geometry. The angular resolution during the analysis was 0.05 degree at a scanning speed of 1 degree/min.

Energy-dispersive elemental analysis was performed using SEM SUPRA 55 VP at an accelerating voltage of 10 kV. Before imaging, samples were coated with gold.

2.1. General synthesis of ZnBTC

Fifteen different ZnBTC samples were each prepared as follows. Two precursors, a zinc salt and 1,3,5-benzenetricarboxylic acid, were taken in the quantities listed in Table 1 and dissolved under ultrasound in a mixture of three solvents, 1 ml each (see Table 1). After that, the solution mixture was hermetically sealed with a lid with a rubber septum in a 4 ml vial to exclude the interaction with the external environment and create excess pressure in the vial. The solution mixture was heated up to 80 °C and kept for 48 h, after which the reaction mixture was cooled down to room temperature. The formed powder was separated from the mother liquid by filtration, and then it was repeatedly washed 5 times with the same mixture of solvents as the one used for its synthesis (see Table 1). The washed powder was dried in the air.

3. Results and Discussion

The synthesis of MOFs was performed under solvothermal reaction conditions (Scheme 1).

Along with the study of the synthesis conditions effect on ZnBTC structure, we analyzed the solvent composition

 DOI: 10.15826/chimtech.2023.10.1.05

(polarity of the mixed aqueous-organic solvent) and the counterion in the Zn salt composition.

The MOF synthesis process can be affected by the reaction medium due to the polarity of the solvent used. To explore this aspect, several ZnBTC were prepared by solvothermal reactions of the Zn^{2+} ion with the H_3BTC ligand in various solvent systems DMF/H_2O/Dioxane, DMF/H_2O/EtOH, DMF/H_2O/Toluene, DMF/H_2O/PhCl, DMF/H_2O/DMSO, respectively (Table 1).

It is known that the medium polarity (the solvent nature) has a great influence on the course of a chemical reaction. The polarity of the medium during the synthesis of ZnBTC-1–15 was calculated according to the literature data. The solvent mixture of DMSO/DMF/H_2O had the highest polarity (corresponds to samples ZnBTC-5, ZnBTC-10, ZnBTC-15), whilst the solvents mixture of Toluene/DMF/H_2O (corresponds to samples ZnBTC-3, ZnBTC-8, ZnBTC-13) was the least polar of the solvent mixtures presented in Table 2.

In the SEM images (Figure 1a–e), all obtained compounds of ZnBTC-1–5 are mainly needle-shaped agglomerates of crystals in the form of "blowball". This form of ZnBTC crystals was obtained for the first time. According to the literature, ZnBTC is usually characterized by a single rectangular crystal [55–58]. However, SEM failed to detect a fragment with a rectangular topology. Compounds of ZnBTC-3 and ZnBTC-4 (Figure 1c and d), synthesized in the solvent mixtures DMF/H_2O/Tol and DMF/H_2O/PhCl, respectively, did not assemble into a whole "blowball".

Such small differences in the crystalline form of the compounds at the same temperature, synthesis time and type of salt could be explained by use of the different types of synthesis medium. The qualitative and quantitative composition of the compounds was analyzed by energy dispersive X-ray (EDX) spectroscopy (Figure 2a–e).

The SEM images of compounds ZnBTC-6–10 can also be described as needle-shaped crystals (Figure 3a–e), but their «blowball» shape is less pronounced than that of substances ZnBTC-1–5. The morphologies of ZnBTC-1 and ZnBTC-6 are different. The synthesis parameters differed only in the type of salt ($Zn(NO_3)_2{\cdot}2H_2O$ and $ZnSO_4{\cdot}7H_2O$), and the solvent medium was the same (Dioxane/DMF/H_2O). Therefore, it can be assumed that the type of salt (counterion) affects the growth of crystals. This assumption is confirmed by the third ZnBTC-MOF series. ZnBTC-11–15, obtained by the interaction of H_3BTC and $Zn(CH_3COO_2)_2{\cdot}2H_2O$, did not form the "blowball" crystalline agglomerates (Figure 4a–e). All compounds ZnBTC-11–15 are crystalline powders.

The nature of the crystalline phase was studied using PXRD analysis [64]. All diffraction patterns of ZnBTC-1–15 (Figure 1f, 3f and 4f) show an intense diffraction peak at $2\theta = 10°$, which corresponds to the literature data [65], confirming the formation of ZnBTC. The diffraction patterns show no background noise over the entire 2θ range. This confirms the presence of a crystalline phase in the studied compositions.

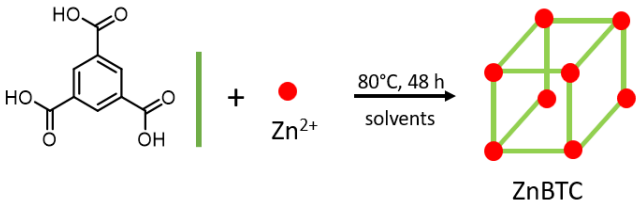

Scheme 1 General synthesis of ZnBTC.

Table 2 Polarity of solvents mixture.

Solvent mixture	Polarity
Dioxane/DMF/H_2O	21.4
EtOH/DMF/H_2O	21.8
Toluene/DMF/H_2O	19
PhCl/DMF/H_2O	19.3
DMSO/DMF/H_2O	23.8

Table 1 Optimization of the synthesis of ZnBTC (Ligand: H_3BTC).

Sample No.	Zn salt	Mixture of solvents (1 ml each)	Ligand/Salt quantities (mmol)
1	$Zn(NO_3)_2{\cdot}6H_2O$	Dioxane/DMF/H_2O	0.067/0.036
2	$Zn(NO_3)_2{\cdot}6H_2O$	EtOH/DMF/H_2O	0.067/0.036
3	$Zn(NO_3)_2{\cdot}6H_2O$	Toluene/DMF/H_2O	0.067/0.036
4	$Zn(NO_3)_2{\cdot}6H_2O$	PhCl/DMF/H_2O	0.067/0.036
5	$Zn(NO_3)_2{\cdot}6H_2O$	DMSO/DMF/H_2O	0.067/0.036
6	$ZnSO_4{\cdot}7H_2O$	Dioxane/DMF/H_2O	0.070/0.035
7	$ZnSO_4{\cdot}7H_2O$	EtOH/DMF/H_2O	0.070/0.035
8	$ZnSO_4{\cdot}7H_2O$	Toluene/DMF/H_2O	0.070/0.035
9	$ZnSO_4{\cdot}7H_2O$	PhCl/DMF/H_2O	0.070/0.035
10	$ZnSO_4{\cdot}7H_2O$	DMSO/DMF/H_2O	0.070/0.035
11	$Zn(CH_3CO_2)_2{\cdot}2H_2O$	Dioxane/DMF/H_2O	0.091/0.046
12	$Zn(CH_3CO_2)_2{\cdot}2H_2O$	EtOH/DMF/H_2O	0.091/0.046
13	$Zn(CH_3CO_2)_2{\cdot}2H_2O$	Toluene/DMF/H_2O	0.091/0.046
14	$Zn(CH_3CO_2)_2{\cdot}2H_2O$	PhCl/DMF/H_2O	0.091/0.046
15	$Zn(CH_3CO_2)_2{\cdot}2H_2O$	DMSO/DMF/H_2O	0.091/0.046

DOI: 10.15826/chimtech.2023.10.1.05

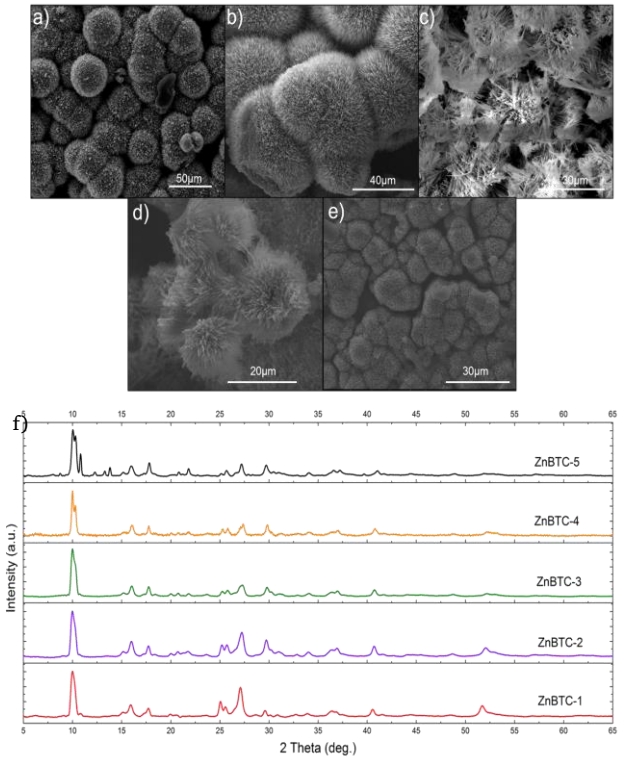

Figure 1 SEM images of ZnBTC-1–5 (a–e, respectively), comparative diffraction pattern of samples ZnBTC-1–5 (f).

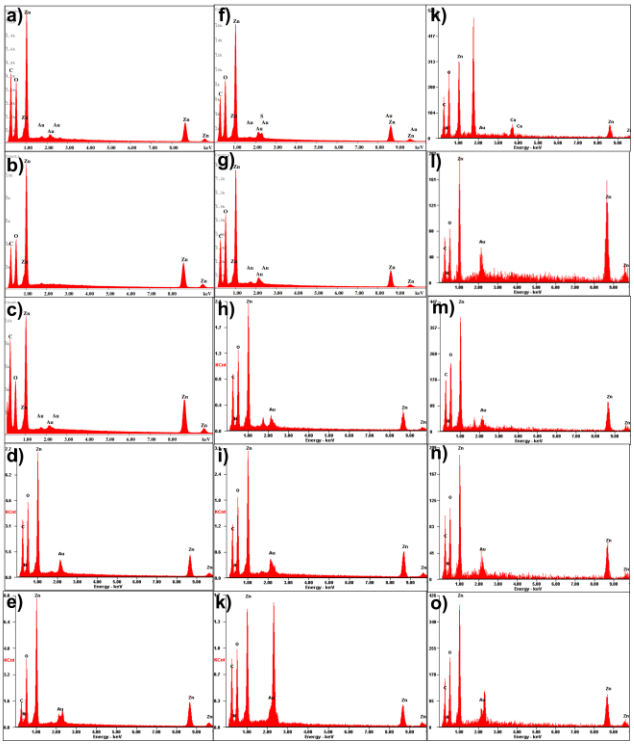

Figure 2 EDX of ZnBTC-1–15 (a–o, respectively).

The appearance of sharp reflections in PXRD patterns indicates a good degree of crystallinity of the synthesized products. The presence of reflections in the region of small angles confirms that the synthesized samples are MOFs. The positions of the main diffraction peaks of all substances ZnBTC-1–15, namely, 10°, 15–20°, 25–30° and 35–40° 2θ (Theta) are identical, which indicates that they possess the same crystal structure.

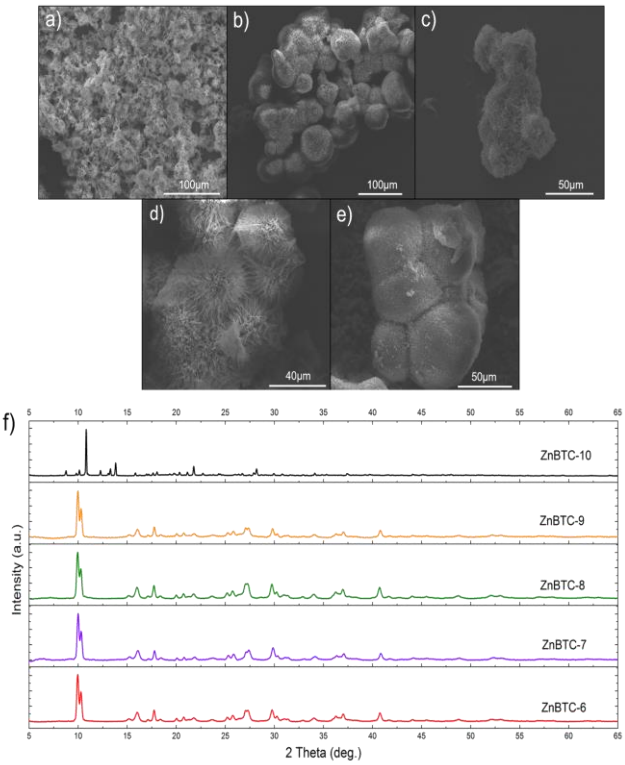

Figure 3 SEM images of ZnBTC-6–10 (a–e, respectively), comparative diffraction pattern of samples ZnBTC-6–10 (f).

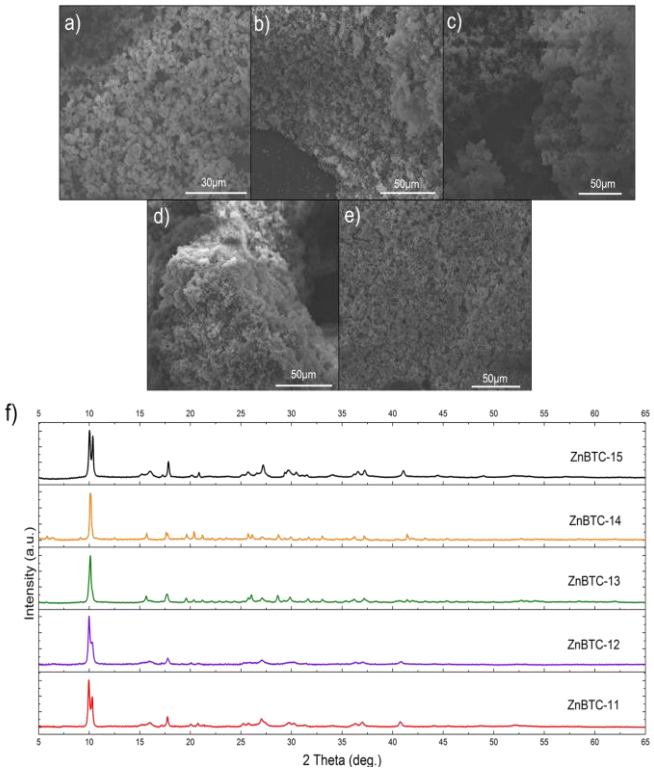

Figure 4 SEM images of ZnBTC-11–15 (a–e, respectively), comparative diffraction pattern of samples ZnBTC-11–15 (f).

But compounds ZnBTC-1–5 also have a diffraction peak at 52° 2θ (Theta) in their PXRD patterns and, in addition, the intensities of the main diffraction peaks of samples ZnBTC-1–5 are greater than those of the other samples. It can be assumed that this is due to the increased crystallinity of the samples ZnBTC-1–5 and the effect of $Zn(NO_3)_2 \cdot 6H_2O$ on the

 DOI: 10.15826/chimtech.2023.10.1.05

crystal growth during synthesis. The diffraction patterns of samples ZnBTC-5 and ZnBTC-10 synthesized in DMSO have additional reflections. It can be assumed that ZnBTC-5 is characterized by a crystal structure different from that of the other ZnBTC.

Comparative analysis of powder diffraction patterns of ZnBTC-1–15 showed that the replacement of the counterion in the composition of the precursor does not affect the elemental composition of MOF and is not included in the structure of the final MOF (Figure 1–4), but the crystallinity and morphology of obtained structures are strongly dependent on the type of salt ($Zn(NO_3)_2 \cdot 6H_2O$ facilitates the formation of more crystalline materials, while $Zn(CH_3CO_2)_2 \cdot 2H_2O$ – of more amorphous, and zinc acetate does not form into "blowball" during the solvothermal synthesis). The reason for this could be that $Zn(NO_3)_2 \cdot 6H_2O$ and $ZnSO_4 \cdot 7H_2O$ are more acidic (pH<7) than $Zn(CH_3CO_2)_2 \cdot 2H_2O$ (pH = 7).

Polarity of the solvent also affects the crystallinity and structure of the obtained compounds. The mixture of DMSO/DMF/H_2O solvents that has the highest polarity among the other ones (Table 2) yields an additional diffraction peak in the region of 10–15° 2θ (Theta) in the PXRD pattern of the synthesized ZnBTC.

4. Limitations

We obtained a new morphology of ZnBTC; therefore, we needed to confirm its structure by single-crystal X-ray crystallography. However, the particles of ZnBTC were agglomerates. The possible solution of this challenge is a recrystallization of a synthesized compound to obtain a single crystal.

5. Conclusions

The results of the study show that the type of solvent and salt does not affect the elemental composition and crystallinity of a ZnBTC-based MOF. However, these critical parameters affect the morphology of the MOF. According to the SEM images, ZnBTC crystals in the form of "blowball" were obtained for the first time. Such sample surface can potentially be used for the sorption of organic molecules.

• Supplementary materials

No supplementary materials are available.

• Funding

This work was supported by the Russian Science Foundation (grant no. 22-23-00738), https://www.rscf.ru/en.

• Acknowledgments

This research would not have been possible without the help of the following organizations:
– Saint Petersburg State Institute of Technology;
– the Faculty of Physics of ITMO;

• Author contributions

Conceptualization: M.V.T., A.N.Y.
Data curation: M.V.T.
Formal Analysis: M.V.T.
Funding acquisition: M.V.T.
Investigation: M.V.T., A.N.Y.
Methodology: M.V.T.
Project administration: M.V.T.
Resources: M.V.T.
Software: M.V.T.
Supervision: M.V.T.
Validation: M.V.T.
Visualization: M.V.T.
Writing – original draft: M.V.T., A.N.Y.
Writing – review & editing: M.V.T.

• Conflict of interest

The authors declare no conflict of interest.

• Additional information

Author IDs:
Maria V. Timofeeva, Scopus ID 57277238300;
Andrey N. Yankin, Scopus ID 56526737600.

Website:
ITMO University, https://itmo.ru.

References

1. Gerasimova EN, Yaroshenko VV, Talianov PM, Peltek OO, Baranov MA, Kapitanova PV, Zyuzin MV. Real-Time temperature monitoring of photoinduced cargo release inside living cells using hybrid capsules decorated with gold nanoparticles and fluorescent nanodiamonds. ACS Appl Mater Interfaces. 2021;13(31):36737–36746. doi:10.1021/acsami.1c05252
2. Gerasimova EN, Yaroshenko VV, Mikhailova LV, Dolgintsev DM, Timin AS, Zyuzin MV, Zuev DA. Thermally induced mechanical switching of the second-harmonic generation in pnipam hydrogels-linked resonant Au and Si nanoparticles. Adv Optic Mater. 2022:2201375. doi:10.1002/adom.202201375
3. Gorrini F, Giri R, Avalos CE, Tambalo S, Mannucci S, Basso L, Bifone A. Fast and sensitive detection of paramagnetic species using coupled charge and spin dynamics in strongly fluorescent nanodiamonds. ACS Appl Mater Interfaces. 2019;11(27):24412–24422. doi:10.1021/acsami.9b05779
4. Gunina E, Zhestkij N, Bachinin S, Fisenko SP, Shipilovskikh DA, Milichko VA, Shipilovskikh SA. The influence of substitutes on the room temperature photoluminescence of 2-amino-4-oxobut-2-enoic acid molecular crystals. Photon Nanostruct Fundament Appl. 2022;48:100990. doi:10.1016/j.photonics.2021.100990

 DOI: 10.15826/chimtech.2023.10.1.05

5. Zhestkij NA, Gunina EV, Fisenko SP, Rubtsov AE, Shipilovskikh DA, Milichko VA, Shipilovskikh SA. Synthesis of highly stable luminescent molecular crystals based on (E)-2-((3-(ethoxycarbonyl)-5-methyl-4-phenylthiophen-2-yl) amino)-4-oxo-4-(p-tolyl) but-2-enoic acid. Chim Techno Acta. 2021;8(4):20218411. doi:10.15826/chimtech.2021.8.4.11
6. Sato O. Dynamic molecular crystals with switchable physical properties. Nat Chem. 2016;8(7):644–656. doi:10.1038/nchem.2547
7. Li J, Jing X, Li Q, Li S, Gao X, Feng X, Wang B. Bulk COFs and COF nanosheets for electrochemical energy storage and conversion. Chemical Society Reviews. 2020;49(11):3565–3604. doi:10.1039/D0CS00017E
8. Fu S, Jin E, Hanayama H, Zheng W, Zhang H, Di Virgilio L, Wang HI. Outstanding charge mobility by band transport in two-dimensional semiconducting covalent organic frameworks. J Am Chem Soc. 2022;144(16):7489–7496. doi:10.1021/jacs.2c02408
9. Illarionov YY, Knobloch T, Grasser T. Inorganic molecular crystals for 2D electronics. Nat Electron. 2021;4(12):870–871. doi:10.1038/s41928-021-00691-w
10. Siddique S, Chow JC. Gold nanoparticles for drug delivery and cancer therapy. Appl Sci. 2020;10(11):3824. doi:10.3390/app10113824
11. Yusran Y, Li H, Guan X, Fang Q, Qiu S. Covalent organic frameworks for catalysis. Energy Chem. 2020;2(3):100035. doi:10.1016/j.enchem.2020.100035
12. Koohsaryan E, Anbia M. Nanosized and hierarchical zeolites: A short review. Chin J Catal. 2016;37(4):447–467. doi:10.1016/S1872-2067(15)61038-5
13. Möller K, Bein T. Mesoporosity – a new dimension for zeolites. Chem Soc Rev. 2013;42(9):3689–3707. doi:10.1039/C3CS35488A
14. Bai R, Song Y, Li Y, Yu J. Creating hierarchical pores in zeolite catalysts. Trends Chem. 2019;1(6):601–611. doi:10.1016/j.trechm.2019.05.010
15. Liang J, Shan G, Sun Y. Catalytic fast pyrolysis of lignocellulosic biomass: Critical role of zeolite catalysts. Renew Sustain Energy Rev. 2021;139:110707. doi:10.1016/j.rser.2021.110707
16. Chen L, Deng Y, Han W, Jiaqiang E, Wang C, Han D, Feng C. Effects of zeolite molecular sieve on the hydrocarbon adsorbent and diffusion performance of gasoline engine during cold start. Fuel. 2022;310:122427. doi:10.1016/j.fuel.2021.122427
17. Mingabudinova LR, Vinogradov VV, Milichko VA, Hey-Hawkins E, Vinogradov AV. Metal–organic frameworks as competitive materials for non-linear optics. Chem Soc Rev. 2016;45(19):5408–5431. doi:10.1039/C6CS00395H
18. Kulachenkov N, Haar Q, Shipilovskikh S, Yankin A, Pierson JF, Nomine A, Milichko VA. MOF-Based Sustainable Memory Devices. Adv Funct Mater. 2022;32(5):2107949. doi:10.1002/adfm.202107949
19. Bachinin S, Gilemkhanova V, Timofeeva M, Kenzhebayeva Y, Yankin A, Milichko VA. Metal-organic frameworks for metal-ion batteries: towards scalability. Chim Techno Acta. 2021;8(3):20210304. doi:10.15826/chimtech.2021.8.3.04
20. Fonseca J, Gong T, Jiao L, Jiang HL. Metal–organic frameworks (MOFs) beyond crystallinity: amorphous MOFs, MOF liquids and MOF glasses. J Mater Chem A. 2021;9(17):10562–10611. doi:10.1039/D1TA01043C
21. Qian Q, Asinger PA, Lee MJ, Han G, Mizrahi Rodriguez K, Lin S, Smith ZP. MOF-based membranes for gas separations. Chem Rev. 2020;120(16):8161–8266. doi:10.1021/acs.chemrev.0c00119
22. Yaghi OM, O'Keeffe M, Ockwig NW, Chae HK, Eddaoudi M, Kim J. Reticular synthesis and the design of new materials. Nat. 2003;423(6941):705–714. doi:10.1038/nature01650
23. Koryakina IG, Bachinin SV, Gerasimova EN, Timofeeva MV, Shipilovskikh SA, Bukatin AS, Zyuzin MV. Microfluidic synthesis of metal-organic framework crystals with surface defects for enhanced molecular loading. Chem Eng J. 2023;452:139450. doi:10.1016/j.cej.2022.139450
24. Kulachenkov N, Barsukova M, Alekseevskiy P, Sapianik AA, Sergeev M, Yankin A, Milichko VA. Dimensionality mediated highly repeatable and fast transformation of coordination polymer single crystals for all-optical data processing. Nano Lett. 2022;22(17):6972–6981. doi:10.1021/acs.nanolett.2c01770
25. Kenzhebayeva Y, Bachinin S, Solomonov AI, Gilemkhanova V, Shipilovskikh SA, Kulachenkov N, Milichko VA. Light-induced color switching of single metal–organic framework nanocrystals. J Phys Chem Lett. 2022;13(3):777–783. doi:10.1021/acs.jpclett.1c03630
26. Gong M, Yang J, Li Y, Zhuang Q, Gu J. Substitution-type luminescent MOF sensor with built-in capturer for selective cholesterol detection in blood serum. J Mater Chem C. 2019;7(40):12674–12681. doi:10.1039/C9TC04399C
27. Furukawa H, Cordova KE, O'keeffe M, Yaghi OM. The chemistry and applications of metal-organic frameworks. Sci. 2013;341(6149):1230444. doi:10.1126/science.1230444
28. Hong DH, Shim HS, Ha J, Moon HR. MOF-on-MOF architectures: applications in separation, catalysis, and sensing. Bull Kor Chem Soc. 2021;42(7):956–969. doi:10.1107/S0567739476001551
29. Zhao M, Wang Y, Ma Q, Huang Y, Zhang X, Ping J, Zhang H. Ultrathin 2D metal–organic framework nanosheets. Adv Mater. 2015;27(45):7372–7378. doi:10.1002/adma.201503648
30. Bosch M, Yuan S, Rutledge W, Zhou HC. Stepwise synthesis of metal–organic frameworks. Accounts of Chem Res. 2017;50(4):857–865. doi:10.1021/acs.accounts.6b00457
31. Dhakshinamoorthy A, Alvaro M, Horcajada P, Gibson E, Vishnuvarthan M, Vimont A, Garcia H. Comparison of porous iron trimesates basolite F300 and MIL-100 (Fe) as heterogeneous catalysts for lewis acid and oxidation reactions: roles of structural defects and stability. Acs Catal. 2012;2(10):2060–2065. doi:10.1021/cs300345b
32. Rowsell JL, Yaghi OM. Effects of functionalization, catenation, and variation of the metal oxide and organic linking units on the low-pressure hydrogen adsorption properties of metal– organic frameworks. J Am Chem Soc. 2006;128(4):1304–1315. doi:10.1021/ja056639q
33. Ren X, Gao Z, Wu G. Tunable nano-effect of Cu clusters derived from MOF-on-MOF hybrids for electromagnetic wave absorption. Compos Commun. 2022;35:101292. doi:10.1016/j.coco.2022.101292
34. Mat Yusuf SNA, Ng YM, Ayub AD, Ngalim SH, Lim V. Characterisation and evaluation of trimesic acid derivatives as disulphide cross-linked polymers for potential colon targeted drug delivery. Polym. 2017;9(8):311. doi:10.3390/polym9080311
35. So PB, Chen HT, Lin CH. De novo synthesis and particle size control of iron metal organic framework for diclofenac drug delivery. Microporous Mesoporous Mater. 2020;309:110495. doi:10.1016/j.micromeso.2020.110495
36. Guo H, Zhang H, Wu N, Pan Z, Li C, Chen Y, Yang W. Trimesic acid-modified 2D NiCo-MOF for high-capacity supercapacitors. J Alloys Compd. 2022;934:167779. doi:10.1016/j.jallcom.2022.167779
37. Jia R, Zhang R, Yu L, Kong X, Bao S, Tu M, Xu B. Engineering a hierarchical carbon supported magnetite nanoparticles composite from metal organic framework and graphene oxide for lithium-ion storage. J Colloid Interface Sci. 2023;630:86–98. doi:10.1016/j.jcis.2022.10.088
38. Karuppasamy K, Bose R, Vikraman D, Ramesh S, Kim HS, Alhseinat E, Kim HS. Revealing the effect of various organic ligands on the OER activity of MOF-derived 3D hierarchical cobalt oxide@ carbon nanostructures. J Alloys Compd. 2023;934:167909. doi:10.1016/j.jallcom.2022.167909
39. Karuppasamy K, Bose R, Velusamy DB, Vikraman D, Santhoshkumar P, Sivakumar P, Kim HS. Rational design and engineering of metal–organic framework-derived trimetallic nicofe-layered double hydroxides as efficient electrocatalysts for water oxidation reaction. ACS Sustain Chem Eng.

2022;10(45): 14693–14704. doi:10.1021/acssuschemeng.2c02830
40. Zhang X, Liu Z, Qu N, Lu W, Yang S, Tian Y, Zhao Y. Hollow Ni/Co-MOFs with controllable surface structure as electrode materials for high performance supercapacitors. Adv Mater Interfaces. 2022;9(30):2201431. doi:10.1002/admi.202201431
41. Seoane B, Dikhtiarenko A, Mayoral A, Tellez C, Coronas J, Kapteijn F, Gascon J. Metal organic framework synthesis in the presence of surfactants: towards hierarchical MOFs? Cryst Eng Comm. 2015;17(7):1693–1700. doi:10.1039/C4CE02324B
42. Dutta R, Kumar A. Effect of IL incorporation on ionic transport in PVdF-HFP-based polymer electrolyte nanocomposite doped with NiBTC-metal-organic framework. J Solid State Electrochem. 2018;22(9):2945–2958. doi:10.1007/s10008-018-3999-7
43. Wang Z, Ge L, Zhang G, Chen Y, Gao R, Wang H, Zhu Z. The controllable synthesis of urchin-shaped hierarchical superstructure MOFs with high catalytic activity and stability. Chem Commun. 2021;57(70):8758–8761. doi:10.1039/D1CC03547A
44. Zhou M, Tang C, Xia H, Li J, Liu J, Jiang J, Chen C. Ni-based MOFs catalytic oxidative cleavage of lignin models and lignosulfonate under oxygen atmosphere. Fuel. 2022;320:123993. doi:10.1016/j.fuel.2022.123993
45. Sharma K, Kaushik R, Pandey PK, Chowdhury S, Gogoi R, Singh A, Siril PF. Enhanced photocatalytic activity of hierarchical C/ZnO nanocomposite derived from solvothermally restructured Zn-BTC microspheres. J Environ Chem Eng. 2022;10(3):107674. doi:10.1016/j.jece.2022.107674
46. Hu X, Huang T, Zhang G, Lin S, Chen R, Chung LH, He J. Metal-organic framework-based catalysts for lithium-sulfur batteries. Coordinat Chem Rev. 2023;475:214879. doi:10.1016/j.ccr.2022.214879
47. Xu B, Huang Z, Liu Y, Li S, Liu H. MOF-based nanomedicines inspired by structures of natural active components. Nano Today. 2023;48:101690. doi:10.1016/j.nantod.2022.101690
48. Luo Y, Huang G, Li Y, Yao Y, Huang J, Zhang P, Zhang Z. Removal of pharmaceutical and personal care products (PPCPs) by MOF-derived carbons: A review. Sci Total Environ. 2022:159279. doi:10.1016/j.scitotenv.2022.159279
49. Mo Z, Tai D, Zhang H, Shahab A. A comprehensive review on the adsorption of heavy metals by zeolite imidazole framework (ZIF-8) based nanocomposite in water. Chem Eng J. 2022:136320. doi:10.1016/j.cej.2022.136320
50. Jeong C, Ansari Z, Anwer AH, Kim SH, Nasar A, Shoeb M, Mashkoor F. A review on metal-organic frameworks for the removal of hazardous environmental contaminants. Separat Purificat Technol. 2022:122416. doi:10.1016/j.seppur.2022.122416
51. Prasetya N, Wenten IG, Franzreb M, Wöll C. Metal-organic frameworks for the adsorptive removal of pharmaceutically active compounds (PhACs): comparison to activated carbon. Coordinat Chem Rev. 2023;475:214877. doi:10.1016/j.ccr.2022.214877
52. Fu X, Ding B, D'Alessandro D. Fabrication strategies for metal-organic framework electrochemical biosensors and their applications. Coordinat Chem Rev. 2023;475:214814. doi:10.1016/j.ccr.2022.214814
53. Kreno LE, Leong K, Farha OK, Allendorf M, Duyne RPV, Hupp JT. Metal-organic framework materials as chemical sensors. Chem Rev. 2012;112(2):1105–1125. doi:10.1021/cr200324t
54. Jasim SA, Amin HIM, Rajabizadeh A, Nobre MAL, Borhani F, Jalil AT, Khatami M. Synthesis characterization of Zn-based MOF and their application in degradation of water contaminants. Water Sci Technol. 2022;86(9):2303–2335. doi:10.2166/wst.2022.318
55. Zhang D, Shen Y, Ding J, Zhou H, Zhang Y, Feng Q, Zhang P. A Combined experimental and computational study on the adsorption sites of zinc-based MOFs for efficient ammonia capture. Molec. 2022;27(17):5615. doi:10.3390/molecules27175615
56. Anyama CA, Ita BI, Ayi AA, Louis H, Okon EE, Ogar JO, Oseghale CO. Experimental and density functional theory studies on a zinc (II) coordination polymer constructed with 1, 3, 5-benzenetricarboxylic acid and the derived nanocomposites from activated carbon. ACS Omega. 2021;6(43):28967–28982. doi:10.1021/acsomega.1c04037
57. Gupta NK, Bae J, Kim S, Kim KS. Fabrication of Zn-MOF/ZnO nanocomposites for room temperature H2S removal: Adsorption, regeneration, and mechanism. Chemosphere. 2021;274:129789. doi:10.1016/j.chemosphere.2021.129789
58. Linxin D, Song L. Synthesis, structural characterization, methane and nitrogen adsorption of a 3D MOF {(ZnBTC)(CH3) 2NH (2) center dot DMF}(n) with a novel hollow-basket spheral cumulate structure. J Molec Struct. 2021:1223. doi:10.1016/j.molstruc.2020.128871
59. Li S, Yan J, Zhu Q, Liu X, Li S, Wang S, Sheng J. Biological effects of EGCG@ MOF Zn (BTC) 4 system improves wound healing in diabetes. Molec. 2022;27(17):5427. doi:10.3390/molecules27175427
60. Wang Y, Liu Y, Wang H, Dou S, Gan W, Ci L, Yuan Q. MOF-based ionic sieve interphase for regulated Zn^{2+} flux toward dendrite-free aqueous zinc-ion batteries. J Mater Chem A. 2022;10(8):4366–4375. doi:10.1039/D1TA10245A
61. Minh TT, Tu NTT, Van Thi TT, Hoa LT, Long HT, Phong NH, Khieu DQ. Synthesis of porous octahedral ZnO/CuO composites from Zn/Cu-based MOF-199 and their applications in visible-light-driven photocatalytic degradation of dyes. J Nanomater. 2019. doi:10.1155/2019/5198045
62. Tehrani AA, Safarifard V, Morsali A, Bruno G, Rudbari HA. Ultrasound-assisted synthesis of metal–organic framework nanorods of Zn-HKUST-1 and their templating effects for facile fabrication of zinc oxide nanorods via solid-state transformation. Inorg Chem Commun. 2015;59:41–45. doi:10.1016/j.inoche.2015.06.028
63. Jabarian S, Ghaffarinejad A. Simultaneous electrosynthesis of Cu–BTC and Zn–BTC metal-organic frameworks on brass. New J Chem. 2020;44(45):19820–19826. doi:10.1039/D0NJ04304
64. Timofeeva M, Gorbunova I, Alekseevskiy P, Shipilovskikh DA, Shipilovskikh SA. Large scale application of triphenylphosphine oxide thin films for a modified catalytic Appel reaction. Photonics Nanostruct Fundamen Appl. 2022;50:101026. doi:10.1016/j.photonics.2022.101026
65. Zheng Y, Ouyang M, Han X, Lu L, Li J. Investigating the error sources of the online state of charge estimation methods for lithium-ion batteries in electric vehicles. J Power Sources. 2018;377:161–188. doi:10.1016/j.jpowsour. 2018.04.081

 DOI: 10.15826/chimtech.2023.10.1.05